

# PROBING RADIATIVE NEUTRINO MASS MODELS AT THE LHC VIA TRILEPTON EVENTS

DOUNIA CHERIGUI, CHAHRAZED GUELLA

*Department of Physics, University of Sciences and Technology of Oran, BP 1505, Oran, Algeria*

AMINE AHRICHE

*Department of Physics, University of Jijel, PB 98 Ouled Aissa, DZ-18000 Jijel, Algeria*

SALAH NASRI

*Department of physics, United Arab Emirates University, Al-Ain, UAE.*

## Abstract

Trilepton event represents one of the probes of the new physics at high energy colliders. In this talk, we consider the search for processes with final states  $\ell_\alpha^\pm \ell_\beta^\pm \ell_\gamma^\mp + \cancel{E}_T$  where  $\alpha, \beta, \gamma = e, \mu, \tau$ , via the production of singlet charged scalar  $S^\pm$  which arise in a class of radiative neutrino mass models. We discuss the opposite sign same flavor leptons signal, as well as the background free channel in view to get a significant excess at  $\sqrt{s} = 8$  TeV and  $\sqrt{s} = 14$  TeV at the hadron collider LHC.

## 1 Introduction

Accommodating the data from neutrino oscillation experiments required an extension of the standard model of particle with extra degrees of freedom. One of the mechanisms that generate tiny masses for neutrinos,  $m_\nu$ , invoke new physics at the TeV scale where  $m_\nu$  vanishes at the tree level but gets generated at higher loop level<sup>1</sup>. Here, using trilepton events we investigate the possibility of probing a class of models motivated by neutrino mass at the LHC. This class of models contains a singlet charged scalar ( $S^\pm$ ) that decays to charged lepton and neutrino via  $f_{\alpha\beta}$  Yukawa couplings, inducing lepton flavor violating (LFV) processes, whose strength is a subject of severe experimental constraints.

## 2 Model Framework & Space Parameter

In this work, we consider a class of models that contain the following term in the Lagrangian

$$\mathcal{L} \supset f_{\alpha\beta} L_\alpha^T C \epsilon L_\beta S^+ - m_S^2 S^+ S^- + \text{h.c.}, \quad (1)$$

The interactions above induce LFV effects via processes such as  $\mu \rightarrow e\gamma$  and  $\tau \rightarrow \mu\gamma$ , with the following branching fractions, these two branching ratios should not exceed the upper bounds  $\mathcal{B}(\mu \rightarrow e + \gamma) < 5.7 \times 10^{-13}$ <sup>2</sup> and  $\mathcal{B}(\tau \rightarrow \mu + \gamma) < 4.8 \times 10^{-8}$ <sup>3</sup>. Moreover, a new contribution to the muon's anomalous magnetic moment is induced at 1-loop. Figure. 1 shows the allowed space parameter for the charged scalar mass range  $100 \text{ GeV} < m_S < 2 \text{ TeV}$ , while scanning over the couplings  $f$ 's with the LFV constraints being satisfied.

## 3 Current Constraints on Trilepton Signal at the LHC

The charged charged  $S^\pm$  can be produced at the LHC through the processes associated with different sign different flavor charged leptons at the parton level as shown in Figure. 2, including gauge bosons  $W^+ Z/W^+ \gamma^*$  production as standard model contribution. The subsequent decay of  $S^\pm$  results in trilepton final states and a missing energy. In our analysis we consider just  $\ell = e, \mu$ , and use CalcHEP to generate both searched signal and background events.

We look for the event number difference  $N_{ex} = N_M - N_B$ , apply the CMS selection criteria used in<sup>4</sup> to perform our analysis, and then compute the significance of each channel for the set of benchmark points. Figure. 3, shows that it is possible to find at least a  $1\sigma(4\sigma)$  excess in  $20.3 \text{ fb}^{-1}$  ( $300 \text{ fb}^{-1}$ ). These results are consistent with searches for new phenomena

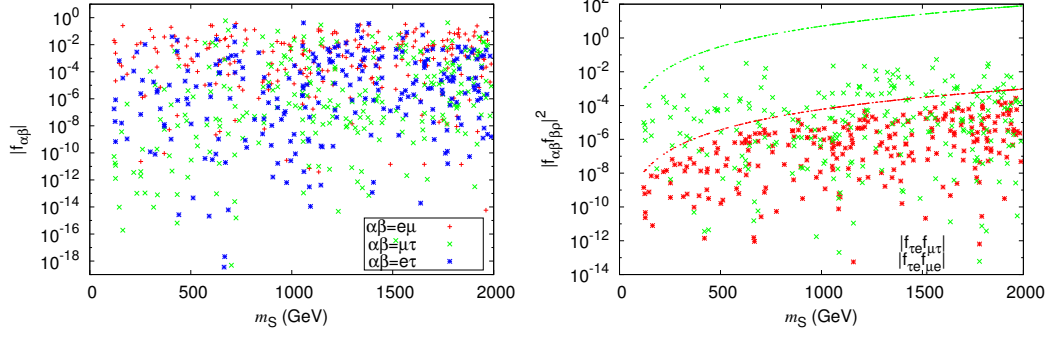


Figure 1 – Different couplings  $f$ 's combinations (as absolute values) versus  $m_S$ , the experimental bounds  $\mu \rightarrow e\gamma$  and  $\tau \rightarrow \mu\gamma$  are represented by dashed lines.

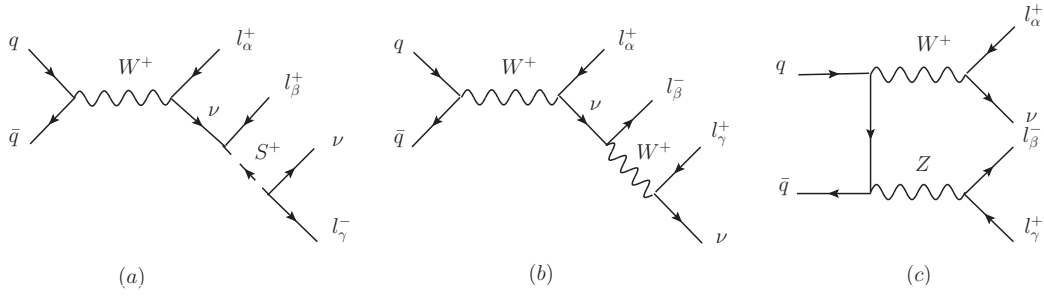


Figure 2 – Diagrams corresponding to the trilepton signal (a) and SM background (b,c).

since they have not shown any significant deviation from SM expectations at 8 TeV. Hence, we will select two benchmark points and apply new cuts for our detailed analysis thereafter in order to perform the significance signal.

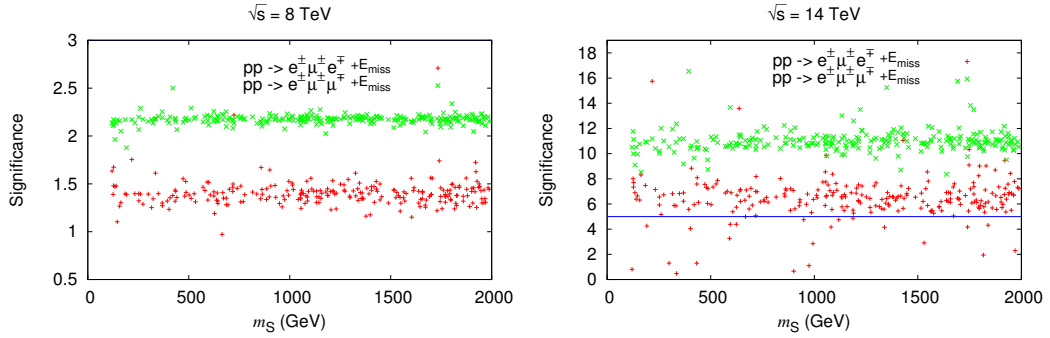


Figure 3 – Significance for the relevant process  $pp \rightarrow \ell^+ \ell^+ \ell^- + \cancel{E}_T$  at 8 TeV (left) and 14 TeV (right), the horizontal blue line indicate the significance value  $S = 5$ .

#### 4 Benchmark Analysis and Discussion

Here, we opt to study the trilepton signal through the two benchmark mass  $B_1$  and  $B_2$  given in Table. 1. We first analyze the trilepton production with opposite sign same flavor final state at  $\sqrt{s} = 8$  and 14 TeV, and then we investigate possibility of observing the background-free signal  $e^+ \mu^+ \tau^-$ .

Table 1: Two benchmark points selected from the allowed parameter space of the model.

Point	$m_S(\text{GeV})$	$f_{e\mu}$	$f_{e\tau}$	$f_{\mu\tau}$
$B_1$	471.8	$-(9.863 + i8.774) \times 10^{-2}$	$-(6.354 + i2.162) \times 10^{-2}$	$(0.78 + i1.375) \times 10^{-2}$
$B_2$	1428.5	$(5.646 + i549.32) \times 10^{-3}$	$-(2.265 + i1.237) \times 10^{-1}$	$-(0.41 - i3.58) \times 10^{-2}$

Table 2: Cuts employed for both processes at  $\sqrt{s} = 8$  TeV and  $\sqrt{s} = 14$  TeV respectively.

$e^+\mu^+e^- + \cancel{E}_T$	$e^+\mu^+e^- + \cancel{E}_T$	$e^+\mu^+\mu^- + \cancel{E}_T$	$e^+\mu^+\mu^- + \cancel{E}_T$
$70 < M_{e^-e^+} < 110$	$70 < M_{e^-e^+} < 110$	$80 < M_{\mu^-\mu^+} < 100$	$80 < M_{\mu^-\mu^+} < 110$
$M_{e^+\mu^+} < 200$	$M_{e^+\mu^+} < 230$	$M_{e^+\mu^+} < 200$	$M_{e^+\mu^+} < 230$
$M_{e^-\nu} < 206$	$M_{e^-\nu} < 220$	$M_{\mu^-\nu} < 185$	$M_{\mu^-\nu} < 245$
$10 < p_T^\ell < 100$	$10 < p_T^\ell < 90$	$10 < p_T^\ell < 100$	$10 < p_T^\ell < 130$
$ \eta^\ell  < 3$	$ \eta^\ell  < 3$	$ \eta^\ell  < 3$	$ \eta^\ell  < 3$
$\cancel{E}_T < 100$	$\cancel{E}_T < 90$	$\cancel{E}_T < 90$	$\cancel{E}_T < 120$

#### 4.1 The Processes $ee\mu$ & $e\mu\mu$

To examine the signal discrimination, we focus on the selected points which are expected to have a favorable cross sections at the LHC. These points motivate us to the investigation of new cuts on the relevant observables as shown in Table. 2, that would be effective in reducing the backgrounds contribution at  $\sqrt{s} = 8$  and 14 TeV, where the processes  $pp \rightarrow \ell^+\ell^+\ell^- + \cancel{E}_T$  are mediating by the Feynman diagrams which can be classified as SM and non-SM diagrams with amplitudes  $\mathcal{M}_{SM}$  and  $\mathcal{M}_S$ , respectively. Therefore,  $N_{ex} = N_M - N_B$  is directly proportional to the couplings combination  $|f_{\alpha\rho}f_{\beta\rho}|^2$ , which means that there is a direct correlation between the discovery LFV processes and signals. The corresponding significance computed for each benchmark point after imposing cuts is shown in Table. 3. Figure. 4 (left) and (center) exhibits the behavior of the signal significance which translate the favorable feasibility of detecting trilepton events through the  $\mu^+\mu^-$  signature.

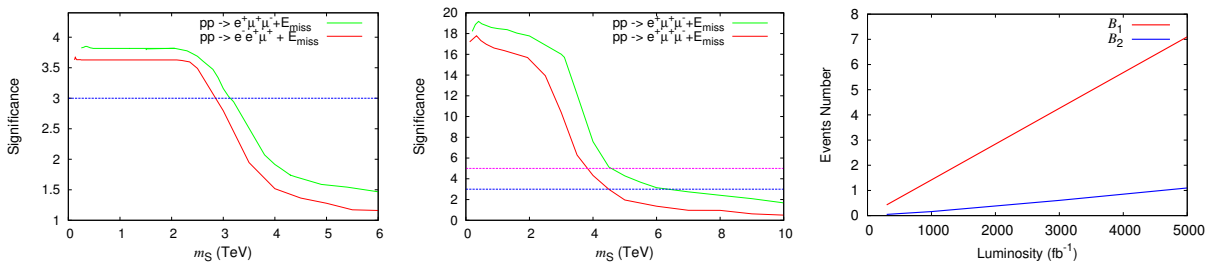


Figure 4 – Significance for the process  $pp \rightarrow \ell^+\ell^+\ell^- + \cancel{E}_T$  at  $\sqrt{s} = 8$  TeV (left) and  $\sqrt{s} = 14$  TeV (center) within new cuts, the dashed horizontal blue (pink) line indicate the significance value  $S = 3$  ( $S = 5$ ) respectively. In (right) events number for the background-free process  $pp \rightarrow e^+\mu^+\tau^- + \cancel{E}_T$  at  $\sqrt{s} = 14$  TeV.

#### 4.2 LFV Background Free Channel

To further our investigation, we extend our earlier analysis in the perspective of optimize the detection of this signature in colliders for both benchmark points through the background free process  $e^+\mu^+\tau^-$ . However, observing such process requires huge luminosity and the resulting number of events is very low (less than 3 events for 1000 fb<sup>-1</sup> luminosity).

Table 3: The significance corresponding to  $\mathcal{L}_{int} = 20.3$  (300)  $fb^{-1}$  at 8 and 14 TeV respectively.

Process	Benchmark	$N_{20.3}$	$S_{20.3}$	$N_{300}$	$S_{300}$
$p, p \rightarrow e^+ \mu^+ e^- + \cancel{E}_T$	$B_1$	70.42	3.651	1689.6	17.363
	$B_2$	69.69	3.618	1470	15.289
$p, p \rightarrow e^+ \mu^+ \mu^- + \cancel{E}_T$	$B_1$	71.21	3.831	2066.7	19.210
	$B_2$	70.44	3.793	1974.9	18.983

#### *Acknowledgments*

D. Cherigui would like to thank the organizers of the Moriond Conference for the financial support.

#### **References**

1. L. M. Krauss, S. Nasri and M. Trodden, Phys. Rev. D **67**, 085002 (2003); M. Aoki, S. Kanemura and O. Seto, Phys. Rev. Lett. **102**, 051805 (2009).
2. J. Adam *et al.* [MEG Collaboration], Phys. Rev. Lett. **110**, 201801 (2013).
3. K. A. Olive *et al.* [Particle Data Group Collaboration], Chin. Phys. C **38**, 090001 (2014).
4. A. Das, P. S. Bhupal Dev and N. Okada, Phys. Lett. B **735**, 364 (2014).